Journal of Power Sources 183 (2008) 240–246

Contents lists available at ScienceDirect

Journal of Power Sources

journal homepage: www.elsevier.com/locate/jpowsour

In situ measurements of water transfer due to different mechanisms in a proton exchange membrane fuel cell

Attila Husar, Andrew Higier, Hongtan Liu*

Department of Mechanical and Aerospace Engineering, University of Miami, Coral Gables, FL 33124, United States

ARTICLE INFO

Article history:
Received 10 March 2008
Received in revised form 7 April 2008
Accepted 8 April 2008
Available online 26 April 2008

Keywords:
PEM
Fuel cell
Water transport
Water management
Electro-osmotic drag

ABSTRACT

Water management is of critical importance in a proton exchange membrane (PEM) fuel cell, in particular, those based on a sulfonic acid polymer, which requires water to conduct protons. Yet there are limited in situ studies of water transfer through the membrane and no data are available for water transfer due to individual mechanisms through the membrane in an operational fuel cell. Thus it is the objective of this study to measure water transfer through the membrane due to each individual mechanism in an operational PEM fuel cell. The three different mechanisms of water transfer, i.e., electro-osmotic drag, diffusion and hydraulic permeation are isolated by specially imposed boundary conditions. Therefore water transfer through the membrane due to each mechanism is measured separately. In this study, all the data is collected in an actual assembled operational fuel cell. The experimental results show that water transfer due to hydraulic permeation, i.e. the pressure difference between the anode and cathode is at least an order of magnitude lower than those due to the other two mechanisms. The data for water transfer due to diffusion through the membrane are in good agreement with some of the ex situ data in the literature. The data for electro-osmosis show that the number of water molecules dragged per proton increases not only with temperature but also with current density, which is different from existing data in the literature. The methodology used in this study is simple and can be easily adopted for in situ water transfer measurement due to different mechanisms in other PEM fuel cells without any cell modifications.

1. Introduction

In a PEM fuel cell, the most commonly used electrolyte is the Nafion® membrane or similar ionomer. Such membranes need to be well-hydrated in order to maintain high proton conductivity. Though water is produced during fuel cell operations, the anode side of the membrane and the anode catalyst layer are often de-hydrated due to the electro-osmotic drag effect. Thus, even though water is a product of a fuel cell, it often must be added to the gas streams to ensure proper hydration of the membrane and catalyst layers. Yet, too much water can cause flooding in the cathode catalyst layer, gas diffusion layers and the channels. Therefore, a delicate water balance is needed to ensure proper operation of a PEM fuel cell using the current membrane technology.

The difficulty of water balance in the PEM fuel cell lies in the interactions of three different mechanisms of water transfer through the membrane, diffusion, hydraulic permeation, and the so called electro-osmotic drag (EOD). Diffusion is caused by the difference in water concentrations between the anode and cathode sides; hydraulic permeation is due to pressure difference between anode and cathode; and EOD occurs when protons pull water molecules when transferring through the membrane. EOD will cause an increase in water content on the cathode side since the protons, and therefore the water, transfers from anode to cathode.

Most studies on water transfer in fuel cells are based on mathematical modeling. In most models, the correlations for water diffusivity and electro-osmotic drag coefficients used were mostly based on one correlation [1], which was based on ex situ measurement of water transfer in the Nafion® 117 membrane. For a Nafion® 117 membrane of 178 μm thickness, pretreated in boiling water, fully hydrated and in equilibrium with liquid water, the number of water molecules dragged per every proton was determined to be 2.5 ± 0.2. For a membrane which is not fully saturated the EOD coefficient was found to be approximately 0.9. Therefore the protonic drag coefficient was determined to be a function of the membrane hydration [2]. In the same study [2], the intra-diffusion coefficient was measured using the pulsed-field gradient spin-echo nuclear magnetic resonance (NMR) technique.

* Corresponding author. Tel.: +1 305 284 2019; fax: +1 305 284 2580.
E-mail address: hliu@miami.edu (H. Liu).

0378-7753/$ – see front matter © 2008 Elsevier B.V. All rights reserved.
doi:10.1016/j.jpowsour.2008.04.042

Nomenclature

A	area
c	water concentration
C	mass fraction
ΔC	water concentration difference
ΔC_m	log mean water concentration difference
D	effective diffusivity
K_m	effective hydraulic permeability
m	mass
$\dot{m}$	mass flow rate
M	molecular weight
n	number of water molecules transferred
p	pressure
q	water mass transfer flux through the membrane
Q	water mass transfer rate through the membrane
t	time

Greek symbols

δ_m	dry membrane thickness
μ	dynamic viscosity
ρ_m	dry membrane density

Subscripts

a	air
d	diffusion
e	exit/outlet
EOD	electro-osmotic drag
hyd	hydraulic permeability
in	inlet
m	membrane
out	outlet
sat	saturation
w	water

Superscripts

a	anode
c	cathode
g	generation

In 2007 Dunbar and Masel [3] used MRI to measure water distribution in an assembled fuel cell using an MEA assembled from a Nafion 115 membrane. This study found that, at low current densities, water was transported from the cathode to the anode signifying that diffusion forces and hydrophobic capillary pressures appeared to dominate over the electro-osmotic forces. Trabold et al. [4] used in situ neutron radiography to investigate how and where water accumulates in a flow field and how different parameters such as humidification of reactants affected the water accumulation.

In 2000 Choi et al. [5] performed experimental studies to determine the net drag coefficient in Nafion 115, which was the resultant water transfer coefficient due to both EOD and diffusion. In 2001 Janssen and Overvelde [6] presented the measured results of the net drag coefficient for a Nafion 112 membrane under a wide range of operating conditions including temperature, pressure, stoichiometry and current density. The net water transfer through the membrane was measured using a condenser after the cell outlets. In 2006 in a study by Yan et al. [7] the net water flux through a Nafion 117 membrane at various temperatures and humidification was measured. This study measured the effects of concentration difference across the membrane as well as pressure difference across the membrane on the net water flux. They found that the net drag coefficient depended on current density and humidification of feed gasses and that the pressure difference across the membrane had less effect on the net water flux than concentration differences and EOD.

All of the above studies are either ex situ measurement of water transfer or measurement of the "net electro-osmotic drag"; what these papers refer to as "net EOD" is actually the net water transfer through the membrane due to both diffusion and EOD. There have been very limited studies focused on water transfer through the membrane due to individual transport mechanisms. Furthermore, water transfer due to EOD will be affected by the catalyst layers since a large volume fraction of the catalyst layer is ionomer. This means that EOD will also occur in the ionomer portion of the catalyst layer. To accurately calculate water diffusion transfer through the membrane, one must use the water contents of the membrane at the anode and cathode sides as boundary conditions. Yet covered with the catalyst layer and the GDL, it is almost impossible to know the water contents at these boundaries. Even though the diffusivity and EOD data for the membrane were accurate, direct application of such data to a real fuel cell may not be appropriate due to the fact that this data was collected ex situ. There is very limited data on water transfer due to hydraulic permeation. Besides, though measurement of total net water transfer through the membrane can be easily performed, such data have limited application to fuel cell design, operation and modeling since water transfer due to the three mechanisms are intertwined.

It is the objective of this study to separately measure water transfer due to the three water transport mechanisms in an operational fuel cell. Through specially imposed conditions, water transfer due to EOD, diffusion and hydraulic permeation were isolated so that in each experiment, water transfer due to only one mechanism could be measured. Such experiments will provide more realistic data for modeling practices. In addition, the applicability of the data obtained is greatly improved because it was obtained in an operational fuel cell.

2. Experimental system

There are four fundamental components in the fuel cell test system used for this study: (1) fuel cell test station, (2) single cell test fixture, (3) fuel cell thermal management system, and (4) reactant gas condenser and water collection equipment. Systematic calibrations were performed on the sub-systems to ensure accuracy of the experimental results. Schematic of the test station can be found in Fig. 1.

The fuel cell test station provides control over the reactant gas humidification temperature and cell operating pressure, as well as anode and cathode mass flow rates. The fuel cell temperature is controlled by an external thermal management system. The reactant gases are humidified by bubbling them through heated water tanks at both the anode and cathode sides. The fuel cell test fixture used in the experiments was designed and manufactured at the University of Miami. The fuel cell flow field used in these experiments was a serpentine single channel design with channel width 1.0 mm, channel height 1.0 mm, land width 1.1 mm and a length of 65.4 mm. The anode and cathode flow fields were identical. The diffusion layers used were carbon fiber cloth material manufactured by E-TEK® known as double-sided ELAT®, i.e. both sides of the carbon fiber cloth were coated with micro-diffusion layers. The catalyst loadings were 0.4 mg cm^{-2} platinum on both the anode and cathode sides. The membrane was Nafion® 115, which has an average thickness of 125 μm and the active area was 50 cm^2.

The temperature of the fuel cell is controlled by a thermal management system, in which the water glycol mixture at a preset

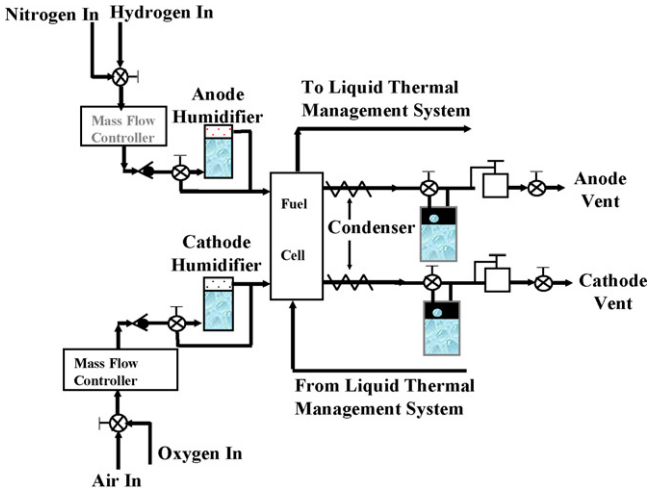

Fig. 1. Schematic of test system.

temperature flows though the cooling channels in the end plates of the cell fixture and the temperature of the fluid is controlled with a thermal bath. An in-house designed water vapor condenser was used to condense both the anode and cathode exit gas streams. In the condenser, the cooling fluid was supplied by an external cooler with a temperature control precision of 0.5 °C. A set of bypass valves were installed before the condenser so that the exit gas streams could be switched easily either going through or bypassing the condenser. The condenser was connected to a cooling loop that uses automotive antifreeze coolant as the working fluid. The coolant loop is set to a constant temperature.

3. Experimental methodologies

The following experiments were designed to separately measure water transfer due to each of the three mechanisms: hydraulic permeation, diffusion and electro-osmotic drag.

3.1. Hydraulic permeation

To isolate hydraulic permeation, water transfer due to both EOD and diffusion must be eliminated. EOD can be eliminated by setting the cell current to zero. Diffusion can be eliminated by ensuring that both the anode and cathode sides have the same water content. This was done by filling the flow channels of both sides with de-ionized (DI) water. It may seem natural to use 100% humidified gas streams on both anode and cathode to measure hydraulic permeation, but such an approach was found to be extremely difficult due to the very large measurement error involved. Since water transfer rate due to hydraulic permeation is extremely low, the amount of water supplied by humidifying the gas streams at the inlets would be orders of magnitude higher than the permeation rate. As a result, the difference in the collected water from the two exit streams in the condenser would be so small that it would be impossible to accurately determine the hydraulic permeation rate. The exit of one side, anode side for example, is connected to the water collecting tube that is open to the atmosphere. The cathode side is pressurized to a pre-determined pressure. The amount of water increased in the anode side water collection tube during a specified period of time is the water transferred due to hydraulic permeation. Before the experiments, rigorous leak-checks of the system have been performed to ensure the accuracy of the experimental results.

3.2. Diffusion

In order to separately measure water transfer due to diffusion only, the effects of EOD and hydraulic permeation must be eliminated. The EOD can again be easily eliminated by setting the cell current to zero and the hydraulic permeation can be eliminated by ensuring both sides have the same pressure. Since, during this set of experiments, water will diffuse from the wet side (the anode side in this study) to the dry side, the water concentration of the wet side will generally decrease and that of the dry side will always increase along the channel. Thus the water concentration difference across the membrane and GDLs cannot be a constant along the channel. Knowledge of water concentration at the two inlets and two outlets can be used to determine the log mean concentration difference across the membrane, as is often used in heat exchanger designs [e.g. 9]. However, with water content varying on both sides, and because water diffusivity through the membrane depends on the water content in the membrane, without proper control of the water contents at these four points the experimental results would have large uncertainties. To improve accuracy, water content on the wet side was maintained constant throughout the cell. This was accomplished by over-saturating the wet side so much that wet side is always over-saturated throughout the cell. For any test run if the outlet gas of the wet side was found not to be over-saturated, the test results would be eliminated. At the dry side, completely dry gas was introduced to maximize water gradient across the membrane and to minimize experimental errors. Furthermore, to maintain consistency the outlet relative humidity was maintained in the vicinity of and less than 50%.

3.3. Electro-osmotic drag

In order to measure water transfer due to electro-osmotic drag, the fuel cell must be generating current and at the same time the driving forces for hydraulic permeation and diffusion must be eliminated. Hydraulic permeation can be easily eliminated by maintaining the same pressure at both the anode and cathode sides. To eliminate diffusion, the water vapor activities, and thus the water content, at both sides must be kept the same throughout the cell. This is achieved by ensuring both sides to be fully humidified throughout the cell at the same temperature. Since water will transfer from the anode side to the cathode side, water content would decrease along the anode channel and increase along the cathode channel. To ensure a fully humidified anode, it must be supplied with over-saturated gas stream and it must be ensured that its humidity level never drop below saturation until the exit. The air in the cathode side was also fully humidified, and the air flow rate was so chosen that excess liquid water must be able to be removed effectively to avoid significant flooding.

4. Results and discussions

In order to determine the amount of water transfer through the membrane the following must be calculated: the amount of water that is brought into the system by each gas stream, the amount of water produced by the reaction, and the amount of water that leaves the system through the two exhaust streams.

4.1. Hydraulic permeation

First, the mass transfer rate of liquid water Q from the higher pressure side (anode) to the lower pressure side (cathode) was measured and then the mass flux q is calculated by dividing Q by the active area of the membrane. From this mass flux q, the effective

permeability of the membrane can be determined from

$$q_{\text{hyd}} = C_{\text{w}} \frac{K_{\text{m}}}{\mu} \frac{\text{d}p}{\text{d}y} \quad (1)$$

where μ is the dynamic viscosity of water, K_{m} is the effective hydraulic permeability of the membrane and C_{w} is the mass fraction of water, which equals 1 here since the anode and cathode channels where filled with liquid water. Since the catalyst layers and the diffusion layers are porous, the values of their permeability must be several orders of magnitude greater than that of the membrane. Therefore, the hydraulic permeability obtained can be used as the effective permeability of the membrane.

The term dp/dy represents the hydraulic pressure difference across the membrane divided by the nominal initial thickness of the membrane. The membrane used was Nafion® 115. Then from Eq. (1) the effective hydraulic permeability of the membrane can be determined from

$$K_{\text{m}} = \frac{q_{\text{hyd}} \delta_{\text{m}} \mu}{\Delta p} \quad (2)$$

where δ_{m} represents the dry membrane thickness provided by the manufacturer, and Δp is the pressure difference between the anode and cathode sides. Mass flux of water is plotted against the pressure difference at three different cell temperatures in Fig. 2. It can be observed that a good linear relationship exists between mass flux and the pressure difference, as expected. It can be seen that the mass flux increases with temperature. Since water uptake of the membrane increases with temperature, there should be more nano-scale water channels [8]. The results of mass flux and hydraulic permeability are shown in Figs. 2 and 3. It can be seen that the hydraulic permeability varies slightly with pressure difference; while it decreases significantly with temperature.

4.2. Water diffusion

In this set of experiments, one side of the fuel cell (the anode) was supplied with nitrogen gas over-saturated with water while on the other side (the cathode) dry air was supplied. Since the inlet water flow rate at the dry side is zero, its exit water flow rate must equal the water transfer rate due to diffusion. This exit water flow rate equals the mass flow rate of water collected in the water trap plus the mass flow rate of water vapor in the exit air leaving the water trap. Assuming the air at the exit of the water trap is saturated

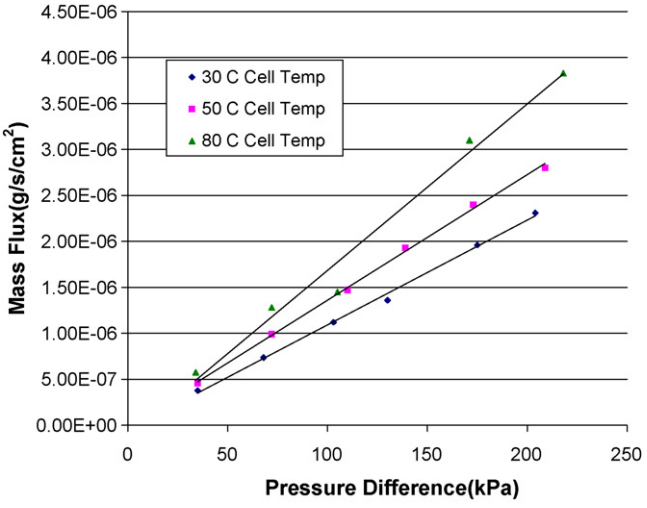

Fig. 2. Water mass transfer flux due to hydraulic permeation through the membrane versus pressure difference at different temperatures.

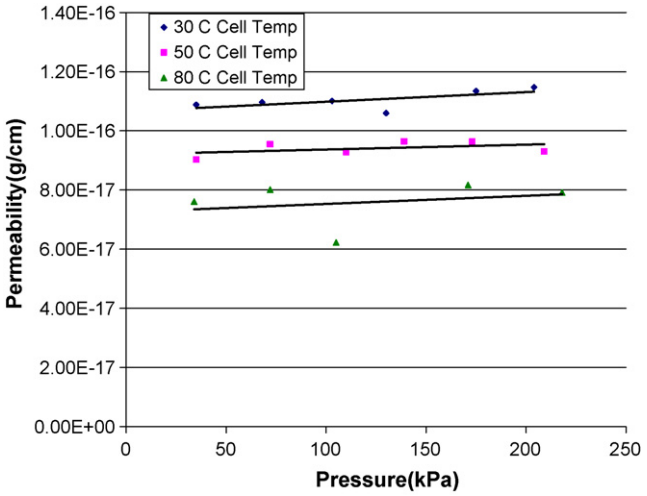

Fig. 3. Hydraulic permeability of water through the membrane at different temperatures.

at the exit temperature, the total water flow rate, thus the water diffusion rate, from the wet side to dry side can be calculated by

$$Q_{\text{d}} = \frac{m_{\text{w}}}{\Delta t} + \dot{m}_{\text{a}} \frac{M_{\text{w}} p_{\text{sat}}}{M_{\text{a}}(p - p_{\text{sat}})} \quad (3)$$

where Q_{d} is the total mass diffusion rate, m_{w} is the mass of water collected in the water trap during the time period of Δt, $\dot{m}_{\text{a}}$ is the dry air mass flow rate and p_{sat} is the vapor saturation pressure at the exit temperature of the water trap. Note that the exit temperature at the water trap was set at 4 °C, therefore the 2nd term in Eq. (3) is very small. Thus, even if the exit gas stream was not 100% saturated the error thus introduced would be extremely small. Once the total mass diffusion rate Q_{d} is obtained, the diffusion mass flux q_{d} can be calculated by dividing it by the cell active area and the effective diffusivity of the membrane can be determined by

$$D = \frac{q_{\text{d}} \delta_{\text{m}}}{\Delta C_{\text{m}}} \quad (4)$$

where δ_{m} is the dry membrane thickness and ΔC_{m} is the log-mean water concentration difference, which can be calculated by

$$\Delta C_{\text{m}} = \frac{\Delta C_{\text{in}} - \Delta C_{\text{out}}}{\ln(\Delta C_{\text{in}} / \Delta C_{\text{out}})} \quad (5)$$

where ΔC_{in} and ΔC_{out} are the water concentration differences between the wet side and the dry side at the inlet and outlet, respectively. The derivation of Eq. (5) is similar to that for the log-mean-temperature-difference (LMTD) used in heat exchanger designs [e.g. 9].

To calculate the water concentrations in the membrane the following correlation [10] was used:

$$c_{\text{w}} = \frac{\rho_{\text{m}}}{M_{\text{m}}} [0.043 + 17.8 a_{\text{w}} - 39.85 a_{\text{w}}^2 + 36.0 a_{\text{w}}^3], \quad 0 \le a_{\text{w}} \le 1 \quad (6)$$

where a_{w} is the water-vapor activity, ρ_{m} is the density of the dry membrane, and M_{m} is the equivalent weight of the dry membrane. Assuming the gas mixture is an ideal gas, the water vapor activity, denoted as a, can be replaced by the relative humidity. The exit gas of the wet side was also condensed and water mass flow rate determined. This was done to ensure that the wet side was kept over-saturated all the way to the exit. Data from any test runs with the wet side exit gas not fully saturated were removed. The diffusivities at different temperatures and different pressures are presented in Figs. 4 and 5. It can be seen from Figs. 4 and 5, the diffusivity increases with temperature and decreases with pressure.

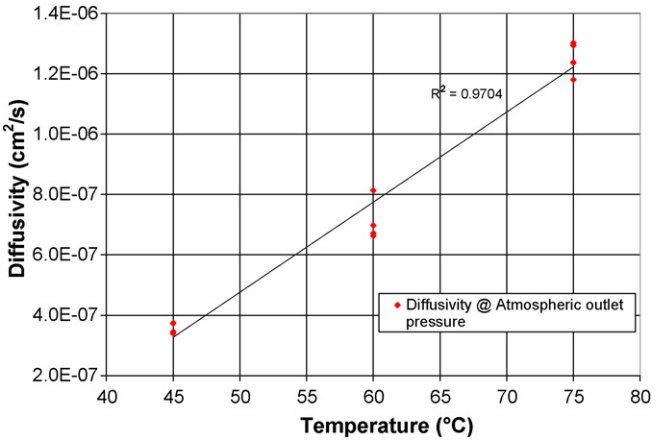

Fig. 4. Variation of effective water diffusivity through the membrane with temperature at atmospheric pressure.

Empirical equations for the diffusion coefficients have been proposed by Springer et al. [1], Nguyen and White [10], and Fuller and Newman [11], etc. However, the values of these coefficients vary widely. It is found that the results based on the correlations from Fuller and Newman [11] are at least an order of magnitude greater than all the others. Thus the measured results are compared only with those from Springer et al. [1] and Nguyen and White [10], as shown in Figs. 6–9. The best comparisons are with the results obtained from the correlation by Nguyen and White [10].

4.3. Results on electro-osmotic drag

In this set of experiments, the mass transfer rate through the membrane can be calculated from the water balance of the anode or the cathode. In this study, the mass transfer rates were calculated from the average of the results obtained from the anode and the cathode to minimize errors. For the anode side, the net water transfer rate equals to the inlet water mass flow rate minus the total outlet water mass flow rate. The total outlet water mass flow rate equals the mass of water collected in the water trap divided by the time period plus the water vapor mass flow rate from the exit of the water trap. It was also assumed that the gases that exited the water traps were fully saturated at the outlet. Thus the water mass flux due to electro-osmotic drag can be obtained as

$$q^{a}_{EOD} = \frac{\dot{m}^{a}_{i} - m^{a}_{w}/\Delta t - \dot{m}^{a}_{e}}{A} \quad (7)$$

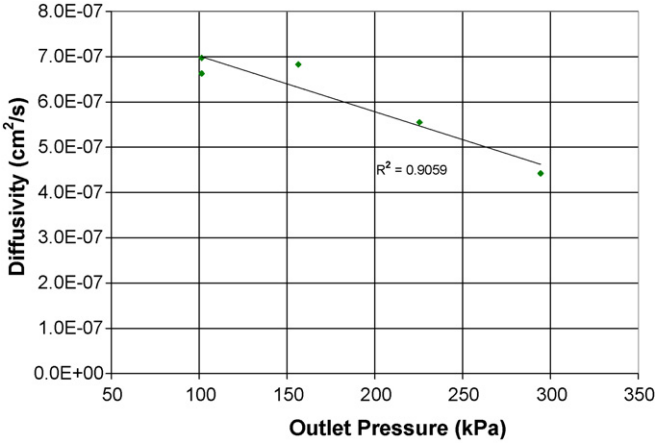

Fig. 5. Variation of effective water diffusivity through the membrane with pressures at 60 °C.

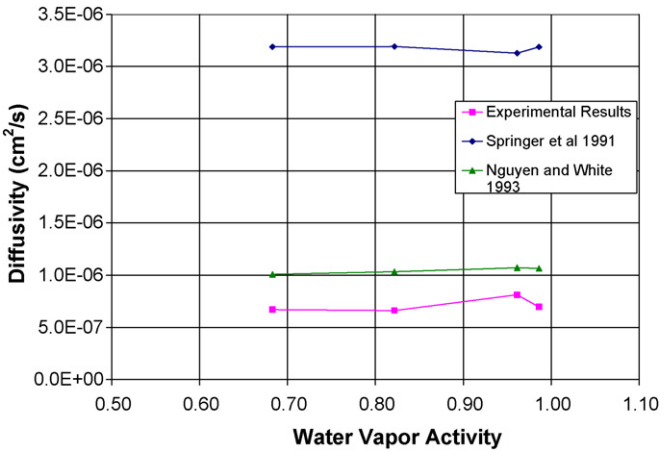

Fig. 6. Comparison of effective water diffusivity at different average water vapor activities at 60 °C.

where $\dot{m}^{a}_{i}$ is water inlet mass flow rate in the humidified hydrogen stream, m^{a}_{w} is the mass of water collected in the anode water trap during the time period of Δt, and $\dot{m}^{a}_{e}$ is the mass flow rate of water from the outlet of the anode water trap.

For the cathode side, similar calculations can be performed. However the water generation rate in the fuel cell must be taken

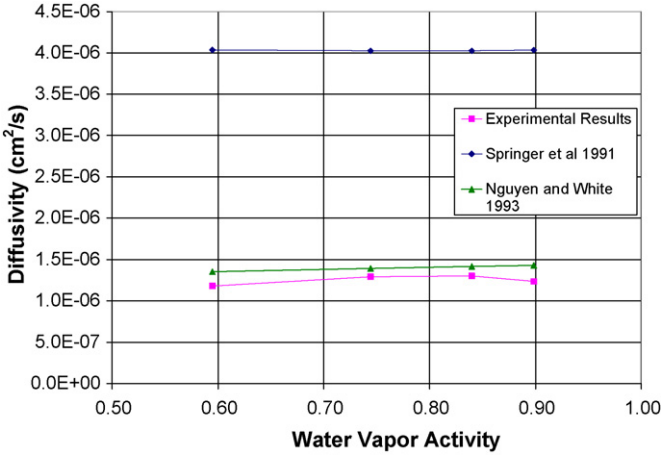

Fig. 7. Average water vapor activity vs. diffusivity comparisons at 75 °C.

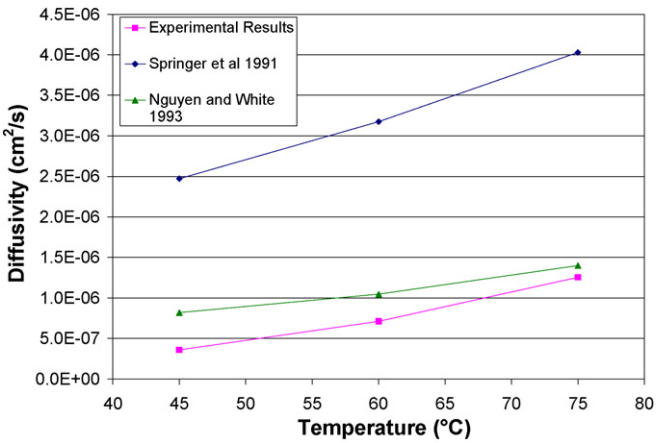

Fig. 8. Comparison of water diffusivity at different temperatures, at pressure 101 kPa.

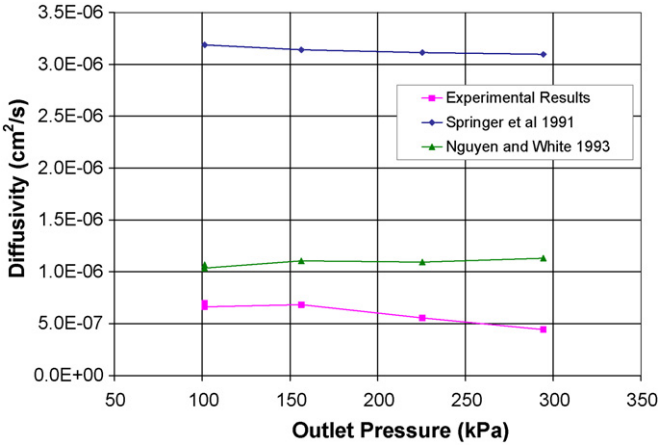

Fig. 9. Comparison of effective water diffusivity at different pressures.

into consideration, thus

$$q^{c}_{EOD} = \frac{m^{c}_{w}/\Delta t + \dot{m}^{c}_{e} - (\dot{m}^{c}_{i} + \dot{m}_{g})}{A} \quad (8)$$

where $\dot{m}^{c}_{i}$ is water inlet mass flow rate in the humidified air stream, $\dot{m}_{g}$ is the water generation rate in the fuel cell and can be calculated from the total cell current, m^{c}_{w} is the mass of water collected in the cathode water trap during the time period of Δt, and $\dot{m}^{c}_{e}$ is the mass flow rate of water from the outlet of the cathode water trap. As mentioned above, to minimize uncertainties, the final effective water mass transfer flux due to EOD is taken to be the average of the results from anode and cathode sides

$$q_{EOD} = \frac{1}{2}(q^{a}_{EOD} + q^{c}_{EOD}) \quad (9)$$

Since for every two protons transferred through the membrane, one water molecule is generated, the number of water molecules transferred due to EOD per proton transferred can be determined by

$$n_{EOD} = \frac{2q_{EOD}}{\dot{m}_{g}} \quad (10)$$

Fig. 10 shows variations of the water mass flux due to EOD as function cell current density at two different temperatures of 40 °C and 60 °C. Data at higher cell temperatures could not be obtained since at higher temperatures, the anode exit gas stream could not

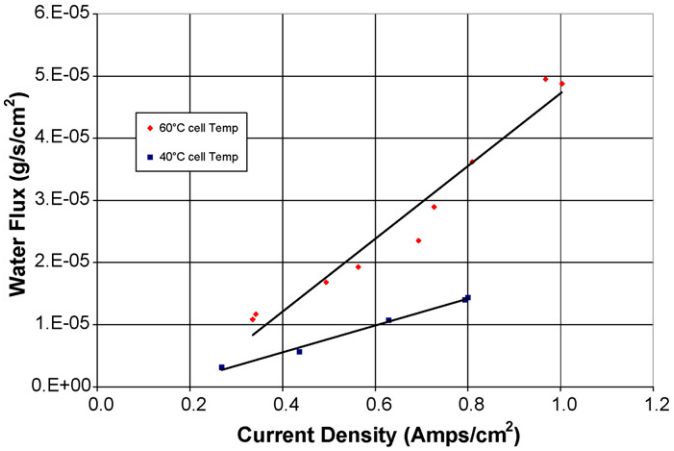

Fig. 10. Variations of effective water flux through the membrane due to electro-osmotic drag with current density at different temperatures.

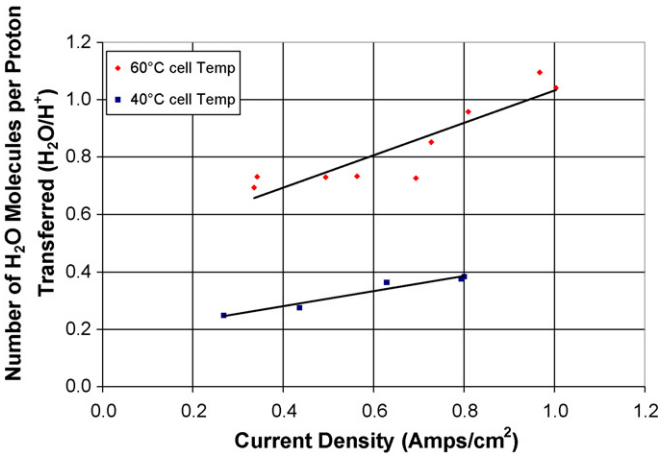

Fig. 11. Number of water molecules transferred through the membrane per proton due to electro-osmotic drag at different current densities.

be maintained fully saturated even if the anode inlet humidification temperature was set at the highest level. From Fig. 10 it can be observed that the water transfer flux due to electro-osmotic drag is much higher at higher temperatures and the rate of increase with current density is also higher at higher temperatures. This is reasonable since EOD depends on the water content in the membrane, which increases with temperature.

Fig. 11 shows the results of number of water molecules transferred per proton. The classical work by Springer et al. [1] and Zawodzinski et al. [2] showed that for fully hydrated (immersed) Nafion® 117 membranes, a drag coefficient was between 2.5 and 2.9. With a partially hydrated membrane, the drag coefficient was determined to be 0.9. It can be seen that the experimental results from this study for 60 °C is in good agreement with their results. Note that the membrane used for this study was Nafion 115 while Zawodzinski et al. [2] used Nafion 117. However, Figs. 10 and 11 show that the electro-osmotic drag coefficient depends strongly on the cell current density as well as on temperature. The fact that the electro-osmotic drag coefficient increases with current density may indicate that our understanding of this phenomenon is not complete and there is a need to revisit the fundamental mechanisms.

5. Concluding remarks

The three different mechanisms of water transfer in an operational PEM fuel cell, i.e., electro-osmotic drag, diffusion and hydraulic permeation were isolated by specially imposed boundary conditions and thus in situ measurements of water transfer due to each individual mechanism were obtained. The measured results showed that water transfer due to hydraulic permeation, i.e. the pressure difference between the anode and cathode is at least an order of magnitude lower than those due to other two mechanisms. The measured effective diffusivity results compared well the correlation by Nguyen and White [10] and the results showed that the effective diffusivity increases with temperature and decreases with pressure. The experimental data on electro-osmosis compared relatively well with the ex situ measurement results for the membrane alone [1,2]. However, the data for electro-osmosis show that the number of water molecules dragged per proton increases not only with temperature but also with current density, which is different from existing data in the literature. The methodology used in this study is simple and can be easily adopted for in situ water transfer measurement due to different mechanisms in different PEM fuel cells without any cell modifications.

References

[1] T.E. Springer, T.A. Zawodzinski, S. Gottesfeld, J. Electrochem. Soc. 138 (8) (1991) 2334–2342.
[2] T.A. Zawodzinski, et al., J. Electrochem. Soc. 140 (4) (1993) 1041–1047.
[3] Z. Dunbar, R.I. Masel, J. Power Sources 171 (2007) 678–687.
[4] T.A. Trabold, J.P. Owejan, D.L. Jacobson, M. Arif, P.R. Huffman, Int. J. Heat Mass Transfer 49 (2006) 4712–4720.
[5] K.-H. Choi, D.-H. Peck, C.S. Kim, D.-R. Shin, T.-H. Lee, J. Power Sources 86 (2000) 197–201.
[6] G.J.M. Janssen, M.L.J. Overvelde, J. Power Sources 101 (2001) 117–125.
[7] Q. Yan, H. Toghiani, J. Wu, J. Power Sources 158 (2006) 316–325.
[8] A.Z. Weber, Newman, J. Electrochem. Soc. 150 (2003) A1008.
[9] S. Kakac, H. Liu, Heat Exchangers: Selection, Rating and Thermal Design, 2nd edition, CRC Press, 2002.
[10] T.V. Nguyen, R.E. White, J. Electrochem. Soc. 140 (8) (1993) 2178–2186.
[11] T.F. Fuller, J. Newman, J. Electrochem. Soc. 140 (5) (1993) 1218–1225.